大阪
inter-noise 2011
Osaka Japan September 4-7

3D sound field reproduction using directional microphones

Toshiyuki Kimura[1]

[1] National Institute of Information and Communications Technology (NICT)

2-2 Hikaridai 2-chome, Seika-cho, Soraku-gun, Kyoto 619-0288 JAPAN

ABSTRACT

In this paper, 3D sound field reproduction technique using directional microphones is proposed. This technique is based on wave field synthesis (WFS) technique, in which the 3D sound field of a listening area is reproduced by using directional microphones and loudspeakers placed at the boundary surface of the area. The position of loudspeakers is the same as that of microphones. First, the effects of the directivity of microphones on the accuracy of synthesized wave fronts are evaluated by computer simulation. The results of computer simulation show that unidirectional or shotgun microphones can synthesize accurate wave fronts in the listening area. Second, in order to reproduce the 3D sound field of the listening area even when the loudspeakers are not placed at the boundary surface of the area, inverse filters calculated from acoustic transfer functions between directional microphones and loudspeakers are applied. The results of computer simulation show that the proposed technique can accurately synthesize wave fronts in the listening area.
Keywords: Sound field reproduction, Wave field synthesis, Directional microphone

1. INTRODUCTION

Wave field synthesis (WFS) [1-3] is a 3D sound field reproduction technique that synthesizes wave fronts on the basis of Huygens' principle. In this technique, the original sound in a control area is captured using a microphone array and it is then reproduced in a listening area using a loudspeaker array. The arrays are placed at the boundary surfaces of their respective areas. The positions of the microphones and the loudspeakers are identical in their respective areas. In this technique, information on the position of listeners and the direction faced by them in the listening area is not required; in contrast, this information is required in other sound field reproduction techniques such as binaural [4] and transaural [5] techniques.

The theoretical background of WFS techniques was studied by Berkhout et al [3]. They assumed that the arrays of microphones and loudspeakers were placed in a line, as shown in the left of Figure 1. On the other hand, surround systems such as 5.1ch and 7.1ch are developed for the home theater system [6] and surround systems based on WFS is proposed [7]. In cases, the arrays of microphones and loudspeakers are placed around the control area and the listening area, as in the right of Figure 1.

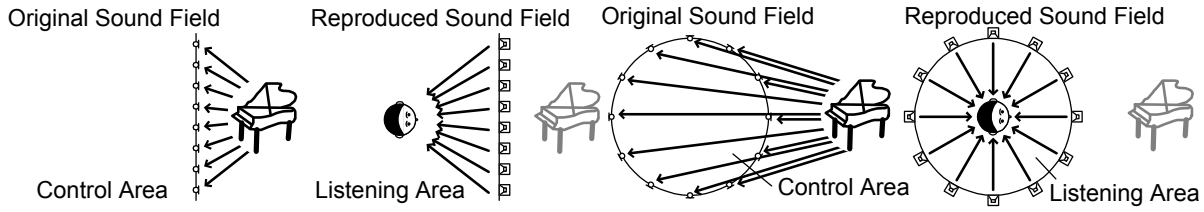

Figure 1 – Original sound field and reproduced sound field

(Left: conventional study, Right: surround system)

The problem is that using the setup shown in the right of Figure 1 can sometimes make the listeners feel they are in a reverberant sound field even though the original sound field is a free field—a field in which there is no reflected sound. This happens when the wave field of a free field is synthesized

[1] t-kimura@nict.go.jp

without using the directivity of microphones so that the sound front comes from all directions in the listening area. If the setup is as in the left of Figure 1, the sound front comes from only the front direction, so the reproduced sound field is not reverberant. Using the directivity of microphones can solve the auditory problem inherent in surround systems set up as in the right of Figure 1.

Although a 3D sound field reproduction technique using directional microphones and WFS was proposed by Camras [2], the effect of microphone directivity was not investigated. In Section 2, the diagram of the proposed technique using WFS is described and the effects of microphone directivity are investigated by using a computer simulation [8-9].

In the 3D sound field reproduction technique using directional microphones and WFS, the loudspeakers are placed on the boundary surface of the listening area. Thus, when visual systems are introduced in the same listening area for an audio-visual presentation, the screen or display of the visual system should be placed on or outside the boundary surface. However, the screen or display cannot be placed on the boundary surface, and the loudspeakers obstruct the audiences' field of view if the screen or display is placed outside the boundary surface. Thus, in order to solve these problems, it is necessary to develop a technique that does not require the positioning of loudspeakers on the boundary surface of the listening area for reproducing the 3D sound field.

In this paper, a 3D sound field reproduction technique using directional microphones and boundary surface control (BoSC) [10] is additionally proposed to reproduce the 3D sound field in the listening area without requiring loudspeakers to be placed at the boundary surface of the area. In Section 3, the diagram of the proposed technique using BoSC is described and a computer simulation is performed and the 3D sound field reproduced in the simulation is numerically analyzed [11].

2. 3D SOUND FIELD REPRODUCTION USING WFS

2.1 Diagram of Proposed Technique

A diagram of the proposed technique is shown in Figure 2. First, in the original sound field, directional microphones are placed on the boundary surface of the control area and the sound is recorded. The directional microphones are then directed toward the outside of the control area. Second, the loudspeaker array is placed in the reproduced sound field and the recorded audio signals are played. The positions of the loudspeakers are the same as those of the directional microphones. As a result, since the 3D sound field is reproduced in the listening area, listeners feel as if they are listening to the sound in the original sound field.

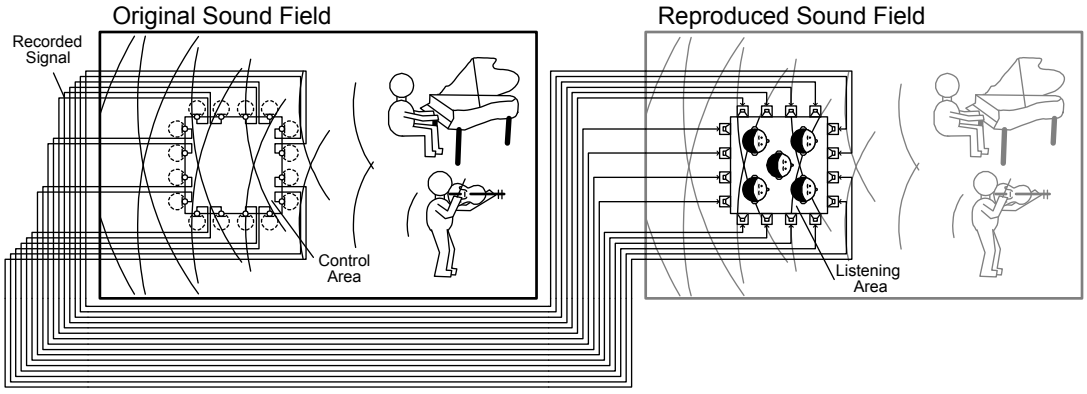

Figure 2 – Diagram of 3D sound field reproduction technique using directional microphones and WFS

2.2 Computer Simulation Condition

The original sound field was assumed to be a free field. The original and reproduced sound fields simulated are shown in Figure 3. The shape of the control and listening areas is a square with sides of $2r$ meters in length. One sound source was placed at the position of d meters and θ degrees azimuth from the center of the control area. Microphones and loudspeakers were arranged along the boundaries of control and listening areas, respectively. Note that the spacing of the microphones and loudspeakers was always constant and the positions of the loudspeakers relative to each other was the same as that of the microphones relative to each other. The directivity of the microphones was toward the outside of the control area. This is the same setup used by Camras [2].

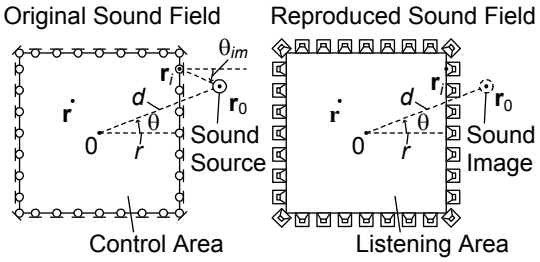

Figure 3 –Sound fields in the computer simulation of the proposed technique using WFS

The sound source signal was a sine-wave signal of frequency f and amplitude A (= $A\sin 2\pi ft$). Let $\mathbf{r}$ be the position vector of an arbitrary point in the control area. Then, $p_0(\mathbf{r},t)$ (sound pressure at $\mathbf{r}$ in original sound field) is denoted as follows,

$$p_0(\mathbf{r},t) = \frac{A}{|\mathbf{r}-\mathbf{r}_0|}\sin\left\{2\pi f\left(t-\frac{|\mathbf{r}-\mathbf{r}_0|}{c}\right)\right\}, \tag{1}$$

where $\mathbf{r}_0$ is the position vector of the sound source and c is the sound velocity. The $x_i(t)$ (recorded signal of the ith microphone) is denoted as follows,

$$x_i(t) = \frac{D_m(\mathbf{r}_0\,|\,\mathbf{r}_i)A}{|\mathbf{r}_i-\mathbf{r}_0|}\sin\left\{2\pi f\left(t-\frac{|\mathbf{r}_i-\mathbf{r}_0|}{c}\right)\right\}, \tag{2}$$

where $\mathbf{r}_i$ and $D_m(\mathbf{r}_0|\mathbf{r}_i)$ are the position vector and the directivity of the ith microphone (i = 1...M), respectively. Note that M is the total number of microphones. The $p(\mathbf{r},t)$ (sound pressure of $\mathbf{r}$ in the reproduced sound field) is calculated as follows,

$$p(\mathbf{r},t) = \sum_{i=1}^{M}\frac{1}{|\mathbf{r}-\mathbf{r}_i|}x_i\left(t-\frac{|\mathbf{r}-\mathbf{r}_i|}{c}\right) = \sum_{i=1}^{M}\frac{D_m(\mathbf{r}_0\,|\,\mathbf{r}_i)A}{|\mathbf{r}-\mathbf{r}_i||\mathbf{r}_i-\mathbf{r}_0|}\sin\left\{2\pi f\left(t-\frac{|\mathbf{r}-\mathbf{r}_i|+|\mathbf{r}_i-\mathbf{r}_0|}{c}\right)\right\}. \tag{3}$$

Table 1 – Parametric conditions in the computer simulation of the proposed technique using WFS

Source frequency f		125, 177, 250, 354, 500, 707, 1000, 1414, 2000, 2828, 4000, 5657, 8000 Hz	
Microphone directivity $D_m(\mathbf{r}_0\|\mathbf{r}_i)$		Omnidirectional, Unidirectional, Shotgun	
Source amplitude A	1	Total number M	800
Source distance d	3, 10, 100 m	Radius of areas r	2 m
Source Azimuth θ	0, 45º	Sound velocity c	340 m/s

Parametric conditions are shown in Table 1. The interval of microphones and loudspeakers is 2 cm, which is less than half of the wavelength of 8000-Hz sound (= 4.25 cm). Thus, the spatial sampling theorem to reproduce the wave front under 8000-Hz sound is satisfied.$\mathbf{r}_0$, $\mathbf{r}$, and $\mathbf{r}_i$ were set as follows,

$$\mathbf{r}_0 = \begin{pmatrix} d\cos\theta & d\sin\theta \end{pmatrix}^T, \quad \mathbf{r} = \begin{pmatrix} r_x & r_y \end{pmatrix}^T \left(|r_x|,|r_y| < r\right), \quad \mathbf{r}_i = \begin{cases} \begin{pmatrix} -r+ri/100 & -r \end{pmatrix}^T & (i=1-200) \\ \begin{pmatrix} r & -r+r(i-200)/100 \end{pmatrix}^T & (i=201-400) \\ \begin{pmatrix} r-r(i-400)/100 & r \end{pmatrix}^T & (i=401-600) \\ \begin{pmatrix} -r & r-r(i-600)/100 \end{pmatrix}^T & (i=601-800) \end{cases}. \tag{4}$$

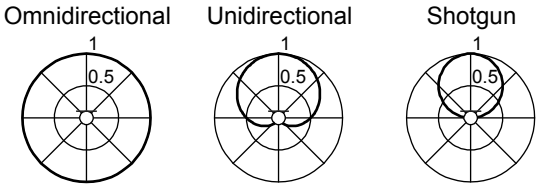

Figure 4 – Directional patterns of microphones

Directional patterns of microphones are shown in Figure 4. The $D_m(\mathbf{r}_0|\mathbf{r}_i)$ (directivity of the ith microphone) is defined as follows,

$$\text{(Omnidirectional) } D_m(\mathbf{r}_0 \mid \mathbf{r}_i) = 1, \quad \text{(Unidirectional) } D_m(\mathbf{r}_0 \mid \mathbf{r}_i) = \frac{1}{2}(1 + \cos\theta_{im}),$$
$$\text{(Shotgun) } D_m(\mathbf{r}_0 \mid \mathbf{r}_i) = \begin{cases} \cos\theta_{im} & (|\theta_{im}| \leq 90^\circ) \\ 0 & (|\theta_{im}| > 90^\circ) \end{cases}, \tag{5}$$

where θ_{im} is the angle between $\mathbf{n}_{im}$ and $\mathbf{r}_{0i}$. Note that $\mathbf{r}_{0i}$ (= $\mathbf{r}_0$–$\mathbf{r}_i$) is the vector from the ith microphone to the sound source and that the $\mathbf{n}_{im}$ (directional vector of the ith microphone) were defined as follows,

$$\mathbf{n}_{im} = \begin{pmatrix} \delta(i-200) & 1 \end{pmatrix}^T (i = 1-200), \quad \mathbf{n}_{im} = \begin{pmatrix} 1 & \delta(i-400) \end{pmatrix}^T (i = 201-400),$$
$$\mathbf{n}_{im} = \begin{pmatrix} -\delta(i-600) & 1 \end{pmatrix}^T (i = 401-600), \quad \mathbf{n}_{im} = \begin{pmatrix} -1 & -\delta(i-800) \end{pmatrix}^T (i = 601-800). \tag{6}$$

2.3 Computer Simulation Result

Results are shown in Figure 5 for simulations run where original wave fronts were t=0 s and f=500 Hz. The synthesized wave fronts and the differences between the original and synthesized wave fronts at t=0 s and f=500 Hz are shown in Figure 6. In these figures, absolute values ($|p_0|$, $|p|$, $|p–p_0|$) of pressures (p_0, p) and differences ($p–p_0$) are plotted and color bars are shown in the right of the figures. The wave fronts are accurately synthesized if the differences are white. Note that the differences are calculated after normalizing the sound pressures (p_0, p) in a space of $|r_x|$, $|r_y|$<1.

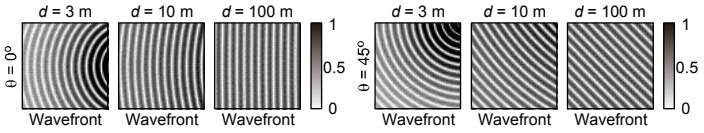

Figure 5 – Wave fronts of original sound field in the proposed technique using WFS (f=500 Hz)

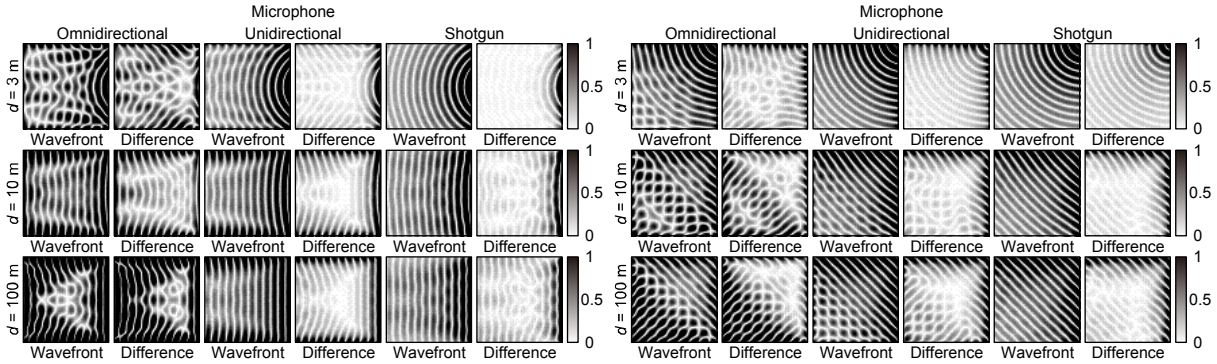

Figure 6 – Synthesized wave fronts and differences in the proposed technique using WFS

(f=500 Hz, Left: θ=0º, Right: θ=45º)

When omnidirectional microphones were used, the wave fronts were not accurately reproduced because the differences were not white. When unidirectional and shotgun microphones were used, the wave fronts were accurately reproduced because the differences of the center of the circles were white.

In order to evaluate quantitatively the reproduced sound field, SNRs (signal-to-noise ratios) were calculated as follows,

$$\text{SNR} = \frac{1}{F}\sum_f \left[10\log_{10} \frac{\sum_{\mathbf{r}} \{p_0(\mathbf{r},0)\}^2}{\sum_{\mathbf{r}} \{p(\mathbf{r},0) - p_0(\mathbf{r},0)\}^2} \right], \tag{6}$$

where F(= 13) is the total number of frequencies. The range of $\mathbf{r}$ is limited to the inside of the 2-m square with ($|r_x|$, $|r_y|$ < 1). Note that $p_0(\mathbf{r},0)$ and $p(\mathbf{r},0)$ were normalized in $|r_x|$, $|r_y|$ < 1 before calculating SNRs.

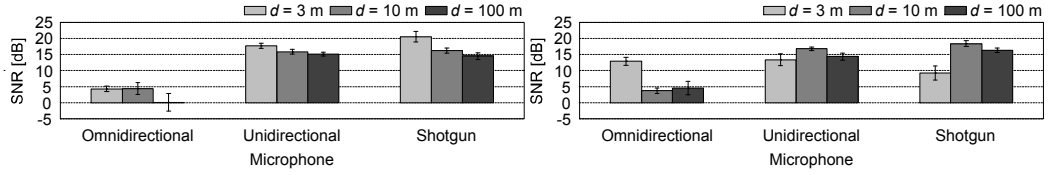

Figure 7 – SNRs in the proposed technique using WFS (Left: θ=0º, Right: θ=45º)

SNR results for the directivity of microphones are shown in Figure 7. Note that error bars denote a

95% confidence interval for SNRs. SNRs of unidirectional and shotgun microphones are higher than those of omnidirectional microphones except in the case of d=3 m, θ=45º. It is thus considered that wave fronts can be accurately reproduced in surround systems based on WFS if unidirectional and shotgun microphones are used.

3. 3D SOUND FIELD REPRODUCTION USING BOSC

3.1 Diagram of Proposed Technique

The diagram of the proposed technique is shown in Figure 8. First, in the original sound field, directional microphones are placed on the boundary surface of the control area and the sound is recorded. The directional microphones are then directed toward the outside of the control area. Second, in the reproduced sound field, directional microphones are placed on the boundary surface of the listening area, and loudspeakers are placed on a boundary surface enveloping the listening area. The position and direction of the directional microphones are the same as those of the microphones during recording. Third, the acoustic transfer functions from the loudspeakers to the directional microphones are measured, and the inverse filters are calculated from the measured acoustic transfer functions. Finally, the recorded signals are filtered by the inverse filters, and the filtered signals are played by the loudspeakers. As a result, since the 3D sound field is reproduced in the listening area, listeners feel as if they are listening to the sound in the original sound field. Since loudspeakers are not placed on the boundary surface of the listening area, it is possible to construct an audio-visual system in which the screen or display of the visual system is placed on or outside the boundary surface of the listening area.

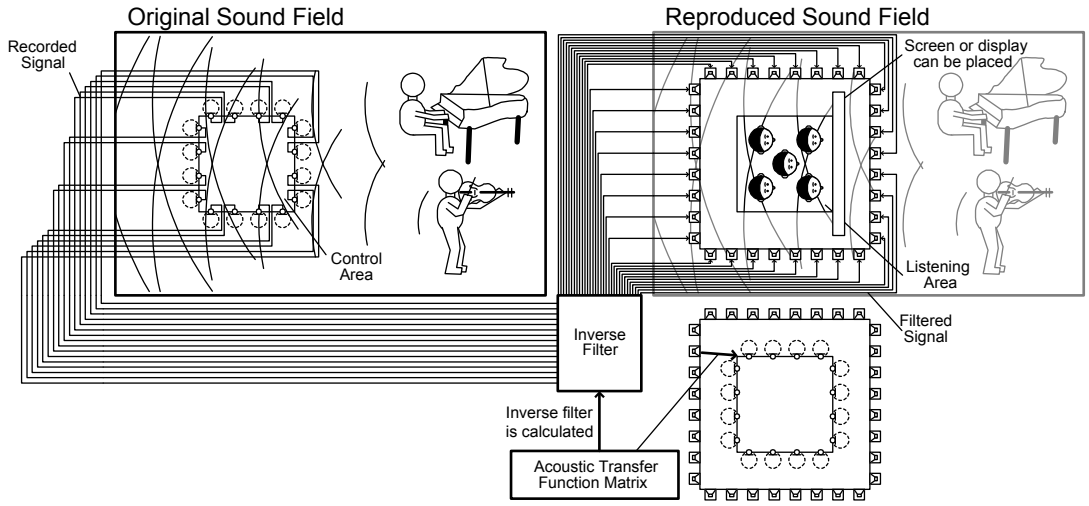

Figure 8 – Diagram of 3D sound field reproduction technique using directional microphones and BoSC

3.2 Computer Simulation Condition

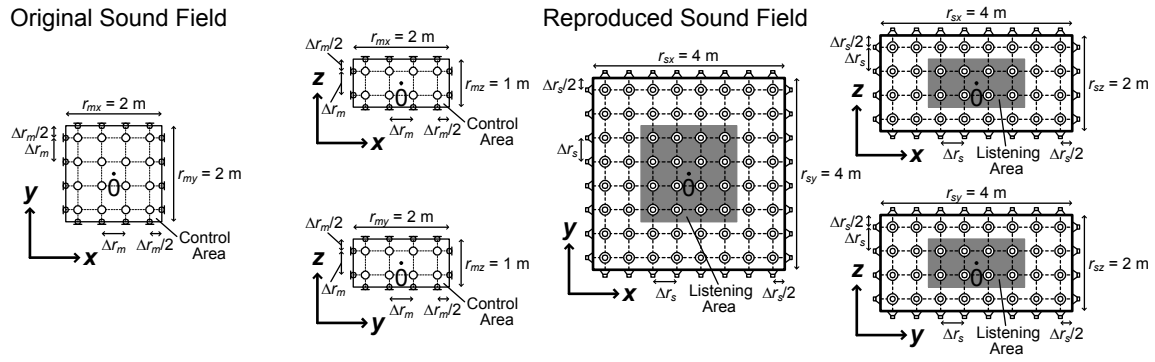

Figure 9 –Sound fields in the computer simulation of the proposed technique using BoSC

The original and reproduced sound fields were formed in free space where there were no reflection sounds.The directional microphone array in the original sound field and the loudspeaker array in the reproduced sound field are shown in Figure 9. The gray shaded area in the reproduced sound field in

Figure 9 denotes the listening area. As shown in Figure 9, directional microphones were placed on six planes of the square prism, with a lattice spacing of Δr_m, and they were directed toward the outside of the control area. Loudspeakers were placed on six planes of the other square prism, with a lattice spacing of Δr_s. The origin of the three-dimensional coordinates was the center of the control and listening areas.

The 3D sound field is reproduced by the proposed technique according to the following steps. First, the $x_i(t)$ (recorded signal of the ith microphone) is recorded according to Eq. (2). The sound source signal is a sinusoidal signal with frequency f and amplitude A ($=A\sin 2\pi ft$). Second, $y_l(t)$ (the filtered signal by using the inverse filter) is denoted as

$$y_l(t) = \sum_{i=1}^{M} \Xi_{li} x_i\left(t - \frac{\Theta_{li}}{2\pi f}\right) = \sum_{i=1}^{M} \frac{\Xi_{li} D_m(\mathbf{r}_0 \mid \mathbf{r}_i) A}{|\mathbf{r}_i - \mathbf{r}_0|} \sin\left\{2\pi f\left(t - \frac{|\mathbf{r}_i - \mathbf{r}_0|}{c}\right) - \Theta_{li}\right\}, \tag{7}$$

where $\Xi_{li}(=|H_{li}(\omega)|)$ and $\Theta_{li}(=\arg H_{li}(\omega))$ denote the absolute value and the angle of the inverse filters. Finally, $p(\mathbf{r},t)$ (the sound pressure at $\mathbf{r}$ in the reproduced sound field) is expressed using the filtered signal $y_l(t)$ by the N loudspeakers placed at $\mathbf{r}'_l$ as follows,

$$p(\mathbf{r},t) = \sum_{l=1}^{N} \frac{1}{|\mathbf{r} - \mathbf{r}'_l|} y_l\left(t - \frac{|\mathbf{r} - \mathbf{r}'_l|}{c}\right) = \sum_{l=1}^{N}\sum_{i=1}^{M} \frac{\Xi_{li} D_m(\mathbf{r}_0 \mid \mathbf{r}_i) A}{|\mathbf{r} - \mathbf{r}'_l||\mathbf{r}_i - \mathbf{r}_0|} \sin\left\{2\pi f\left(t - \frac{|\mathbf{r} - \mathbf{r}'_l| + |\mathbf{r}_i - \mathbf{r}_0|}{c}\right) - \Theta_{li}\right\}. \tag{8}$$

Table 2 – Parametric conditions in the computer simulation of the proposed technique using BoSC

Source frequency f	63, 125, 250, 500, 1000 Hz		
Source direction vector $\mathbf{u}$	$(1,0,0)^T$, $(1/\sqrt{2},1/\sqrt{2},0)^T$, $(2/3,2/3,1/3)^T$		
Microphone interval Δr_m	0.1667 m	Source amplitude A	1
Microphone directivity $D_m(\mathbf{r}_0\|\mathbf{r}_i)$	Shotgun	Source distance d	2, 10, 50 m
Microphone array size r_{mx}, r_{my}, r_{mz}	2×2×1 m	Sound velocity c	340 m/s
Loudspeaker interval Δr_s	0.1667 m	Microphone number M	576
Loudspeaker array size r_{sx}, r_{sy}, r_{sz}	4×4×2 m	Loudspeaker number N	2304

The parametric conditions are listed in Table 2. The microphone interval is 16.67 cm, which is less than half the wavelength of 1000-Hz sound waves (=340/1000=34 cm). Thus, the spatial sampling theorem that pertains to the reproduction of wave fronts of sound waves with frequencies below 1000 Hz is satisfied. $\mathbf{r}_0$, $\mathbf{r}$, $\mathbf{n}_{im}$, $\mathbf{r}_i$ and $\mathbf{r}'_l$ were defined in three-dimensional coordinates as follows,

$$\mathbf{r}_0 = d\,\mathbf{u}, \quad \mathbf{r} = \begin{pmatrix} r_x & r_y & r_z \end{pmatrix}^T (|r_x|, |r_y| < 2, |r_z| < 1), \quad \mathbf{n}_{im} = \begin{cases} \begin{pmatrix} (-1)^i & 0 & 0 \end{pmatrix}^T & (i = 1-144) \\ \begin{pmatrix} 0 & (-1)^{i-144} & 0 \end{pmatrix}^T & (i = 145-288) \\ \begin{pmatrix} 0 & 0 & (-1)^{i-288} \end{pmatrix}^T & (i = 289-576), \end{cases} \tag{9}$$

$$\mathbf{r}_i = \begin{cases} (i = 1-144) & (i = 145-288) & (i = 289-576) \\ \begin{pmatrix} \frac{r_{mx}}{2}(-1)^i \\ \Delta r_m R\left(\frac{i}{2}, \frac{r_{my}}{\Delta r_m}\right) + \frac{\Delta r_m - r_{my}}{2} \\ \Delta r_m Q\left(\frac{i}{2}, \frac{r_{my}}{\Delta r_m}\right) + \frac{\Delta r_m - r_{mz}}{2} \end{pmatrix} & \begin{pmatrix} \Delta r_m R\left(\frac{i-144}{2}, \frac{r_{mx}}{\Delta r_m}\right) + \frac{\Delta r_m - r_{mx}}{2} \\ \frac{r_{my}}{2}(-1)^{i-144} \\ \Delta r_m Q\left(\frac{i-144}{2}, \frac{r_{mx}}{\Delta r_m}\right) + \frac{\Delta r_m - r_{mz}}{2} \end{pmatrix} & \begin{pmatrix} \Delta r_m R\left(\frac{i-288}{2}, \frac{r_{mx}}{\Delta r_m}\right) + \frac{\Delta r_m - r_{mx}}{2} \\ \Delta r_m Q\left(\frac{i-288}{2}, \frac{r_{mx}}{\Delta r_m}\right) + \frac{\Delta r_m - r_{my}}{2} \\ \frac{r_{mz}}{2}(-1)^{i-288} \end{pmatrix} \end{cases}, \tag{10}$$

$$\mathbf{r}'_l = \begin{cases} (l = 1-576) & (l = 577-1152) & (l = 1153-2304) \\ \begin{pmatrix} \frac{r_{sx}}{2}(-1)^l \\ \Delta r_s R\left(\frac{l}{2}, \frac{r_{sy}}{\Delta r_s}\right) + \frac{\Delta r_s - r_{sy}}{2} \\ \Delta r_s Q\left(\frac{l}{2}, \frac{r_{sy}}{\Delta r_s}\right) + \frac{\Delta r_s - r_{sz}}{2} \end{pmatrix} & \begin{pmatrix} \Delta r_s R\left(\frac{l-576}{2}, \frac{r_{sx}}{\Delta r_s}\right) + \frac{\Delta r_s - r_{sx}}{2} \\ \frac{r_{sy}}{2}(-1)^{l-576} \\ \Delta r_s Q\left(\frac{l-576}{2}, \frac{r_{sx}}{\Delta r_s}\right) + \frac{\Delta r_s - r_{sz}}{2} \end{pmatrix} & \begin{pmatrix} \Delta r_s R\left(\frac{l-1152}{2}, \frac{r_{sx}}{\Delta r_s}\right) + \frac{\Delta r_s - r_{sx}}{2} \\ \Delta r_s Q\left(\frac{l-1152}{2}, \frac{r_{sx}}{\Delta r_s}\right) + \frac{\Delta r_s - r_{sy}}{2} \\ \frac{r_{sz}}{2}(-1)^{l-1152} \end{pmatrix} \end{cases}, \tag{11}$$

where $Q(u,v)$ and $R(u,v)$ denote the quotient and remainder when u is divided by v.

3.3 Computer Simulation Result

Results are shown in Figure 10 for simulations run where original wave fronts were t=0 s and f=500 Hz. The wave fronts synthesized by the proposed techniques using WFS (according to Eq. (3)) and BoSC (according to Eq. (8)) and the differences between the original and synthesized wave fronts at t=0 s and f=500 Hz are shown in Figure 11. In these figures, only the XY plane (z=0), XZ plane (y=0), and YZ plane (x=0) in the space surrounded by the loudspeaker array (4 m×4 m×2 m) are plotted, and the dashed lines denote the boundary of the listening area (2 m×2 m×1 m) surrounded by the loudspeaker array. In these figures, absolute values of sound pressures (p_0, p) and the differences (p-p_0) are plotted; color bars are shown on the right side of the figures. The wave fronts in the listening area are accurately synthesized if the differences are white. Note that the differences are calculated after normalizing the sound pressures (p_0, p) in a space with dimensions of 1 m (width) × 1 m (depth) × 0.5 m (height) in the listening area (i.e., $|r_x|$, $|r_y|$<0.5, $|r_z|$<0.25).

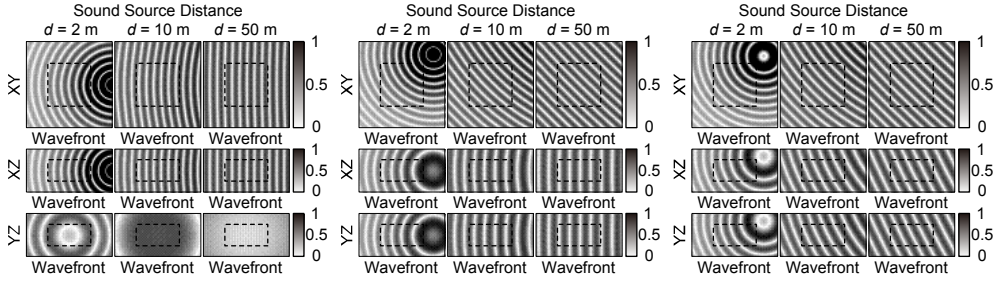

Figure 10 – Wave fronts of original sound field in the proposed technique using BoSC (f=500 Hz, Left: $\mathbf{u}=(1,0,0)^T$, Center: $\mathbf{u}=(1/\sqrt{2},1/\sqrt{2},0)^T$, Right: $\mathbf{u}=(2/3,2/3,1/3)^T$)

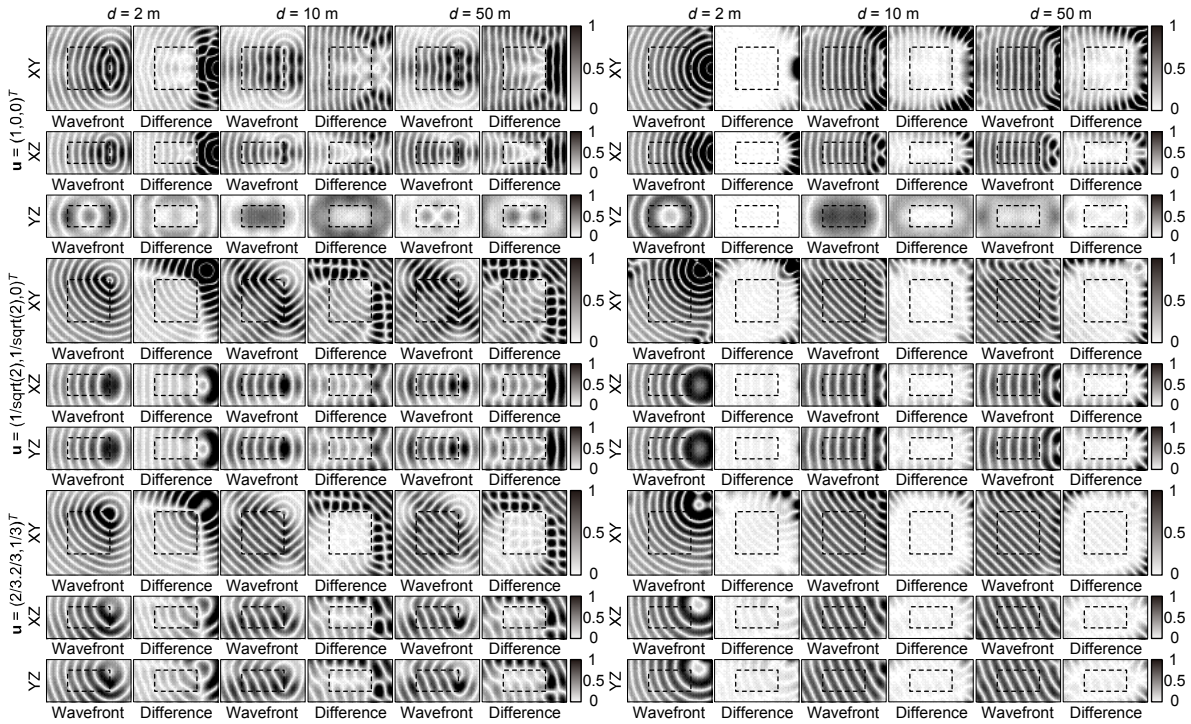

Figure 11 – Synthesized wave fronts and differences in the proposed technique using BoSC (f=500 Hz, Left: proposed technique using WFS, Right: proposed technique using BoSC)

When the proposed technique using WFS is used, the wave fronts are not accurately reproduced, as is evident from the differences not being white. On the other hand, when the proposed technique using BoSC is used, the wave fronts are accurately reproduced, as is apparent from the differences being white. Thus, the proposed technique using BoSC can reproduce wave fronts more accurately than the proposed technique using WFS.

In order to quantitatively evaluate the reproduced sound field, SNRs (signal-to-noise ratios) were calculated as follows,

$$\mathrm{SNR} = 10\log_{10}\frac{\sum_f \sum_{\mathbf{r}} \{p_0(\mathbf{r},0)\}^2}{\sum_f \sum_{\mathbf{r}} \{p(\mathbf{r},0) - p_0(\mathbf{r},0)\}^2}, \tag{12}$$

where the range of $\mathbf{r}$ was limited to the space with dimensions of 2 m×2 m×1 m (i.e., $|r_x|$, $|r_y|$<1, $|r_z|$<0.5). Note that $p_0(\mathbf{r},0)$, $p(\mathbf{r},0)$ were normalized in the range described above before calculating the SNRs.

The SNR values for each system are shown in Figure 12. The values for the proposed technique using WFS are always lesser than 5 dB for all source distances and directions. On the other hand, in the proposed technique using BoSC, the SNRs are always greater than 10 dB and exceed the values for the proposed technique using WFS by more than 7 dB for all source distances and directions. It is thus inferred that wave fronts can be accurately reproduced in the proposed technique using BoSC.

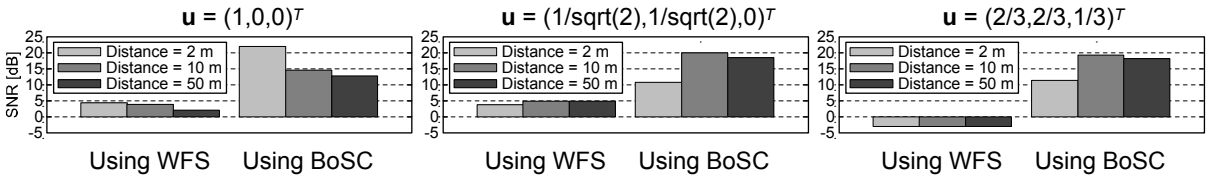

Figure 12 – SNRs in the proposed technique using WFS and BoSC

4. CONCLUSION

In this paper, 3D sound field reproduction technique using directional microphones was proposed. This technique was based on wave field synthesis (WFS). First, the effects of the directivity of microphones were evaluated by computer simulation. The results of computer simulation showed that unidirectional or shotgun microphones could synthesize accurate wave fronts in the listening area. Second, in order to reproduce the 3D sound field even when the loudspeakers were not placed at the boundary surface of the area, 3D sound field reproduction technique using boundary surface control (BoSC) was proposed. This system was constructed by using the inverse filters calculated from acoustic transfer functions between directional microphones and loudspeakers in the WFS technique. The results of computer simulation showed that the proposed technique using BoSC could synthesize more accurate wave fronts than the proposed technique using WFS in the listening area.

REFERENCES

[1] H. Fletcher, “Symposium on wire transmission of symphonic music and its reproduction on auditory perspective: Basic requirement,” Bell Sys. Tech. J., 13(2), 239-244 (1934).

[2] M. Camras, “Approach to recreating a sound field,” J. Acoust. Soc. Am., 43(6), 1425-1431 (1968).

[3] A. J. Berkhout, D. de Vries, P. Vogel, “Acoustic control by wave field synthesis,” J. Acoust. Soc. Am., 93(5), 2764-2778 (1993).

[4] J. Blauert, *Spatial Hearing* (372-392, revised edition, MIT Press, Cambridge, Mass. 1997).

[5] M. R. Schroeder, D. Gottlob, K. F. Siebrasse, “Comparative study of european concert halls: Correlation of subjective preference with geometric and acoustic parameters,” J. Acoust. Soc. Am., 56(4), 1195-1201 (1974).

[6] ITU-R Recommendation BS.775-1, “Multichannel Stereophoneic Sound System with and without Accompanying Picture” (1992-1994).

[7] IOSONO GmbH, http://www.iosono-sound.com/.

[8] T. kimura and K. Kakehi, “Effects of directivity of microphones and loudspeakers on accuracy of synthesized wave fronts in sound field reproduction based on wave field synthesis,” Papers AES 13th Regional Convention, No. 0037, 1-8 (2007).

[9] T. Kimura and K. Kakehi, “Effects of Directivity of Microphones and Loudspeakers in Sound Field Reproduction Based on Wave Field Synthesis,” Proc. ICA, No. RBA-15-011, 1-6 (2007).

[10] S. Ise, “A principle of sound field control based on the Kirchhoff-Helmholtz integral equation and the theory of inverse systems,” ACUSTICA - Acta Acustica, 85(1), 78-87 (1999).

[11] T. Kimura, “Theoretical Study and Numerical Analysis of 3D Sound Field Reproduction System Based on Directional Microphones and Boundary Surface Control,” Proc. AES Int. Conf., No. 10-1, 1-10 (2010).